The costs of competition: high social status males experience accelerated epigenetic aging in wild baboons

Jordan A. Anderson[1]†, Rachel A. Johnston[1]†, Amanda J. Lea[2,3,4], Fernando A. Campos[2,5], Tawni N. Voyles[1], Mercy Y. Akinyi[6], Susan C. Alberts[1,2,6], Elizabeth A. Archie[6,7], Jenny Tung[1,2,6,8,*]

[1]Department of Evolutionary Anthropology, Duke University, Durham, North Carolina 27708, USA
[2]Department of Biology, Duke University, Durham, North Carolina 27708, USA
[3]Lewis-Sigler Institute for Integrative Genomics, Carl Icahn Laboratory, Princeton University, Princeton, NJ 08544, USA
[4]Department of Ecology and Evolution, Princeton University, Princeton, NJ 08544, USA
[5]Department of Anthropology, University of Texas at San Antonio, San Antonio, TX 78249, USA
[6]Institute of Primate Research, National Museums of Kenya, Nairobi 00502, Kenya
[7]Department of Biological Sciences, University of Notre Dame, Notre Dame, Indiana 46556, USA
[8]Duke Population Research Institute, Duke University, Durham, NC 27708, USA

†Authors contributed equally to this work
*Correspondence: jt5@duke.edu

Summary

Aging, for virtually all life, is inescapable. However, within species and populations, rates of biological aging (i.e., physical decline with age) vary across individuals. Understanding sources of variation in biological aging is therefore central to understanding the biodemography of natural populations. Here, we constructed a DNA methylation-based predictor of chronological age for a population of wild baboons in which behavioral, ecological, and life history data have been collected for almost 50 years (N = 277 blood samples from 245 individuals, including 30 who were longitudinally sampled). Consistent with findings in humans and model organisms [1-4], DNA methylation patterns exhibit a strong, clock-like association with chronological age, but individuals are often predicted to be somewhat older or younger than their known age. However, the two most robust predictors of lifespan described for this population—cumulative early adversity and social bond strength—do not explain this deviation. Instead, the single most predictive factor is male dominance rank: high-ranking males are predicted to be biologically older than their true chronological age, such that alpha males appear to be nearly a year older than their known age. Longitudinal sampling indicates that males who climb the social hierarchy subsequently look epigenetically "older," likely reflecting the high energetic costs of rank attainment and maintenance in male baboons. Together, our results indicate that environmental effects on survival and epigenetic age can be disjunct, and that achieving high rank for male baboons—the best predictor of reproductive success—imposes physiological costs consistent with a "live fast, die young" life history strategy.

Keywords: Epigenetic age, epigenetic clock, aging, DNA methylation, dominance rank, baboons

Results and discussion

We used a combination of previously published [5] and newly generated reduced-representation bisulfite sequencing (RRBS) data from 245 wild baboons (N = 277 blood samples) living in the Amboseli ecosystem of Kenya [6] to generate a DNA methylation-based age predictor (an "epigenetic clock:" [1, 2]). Starting with a data set of methylation levels for 458,504 CpG sites genome-wide (Figure S1; Table S1), we used elastic net regression to identify a set of 593 CpG sites that accurately predict baboon age to within a median absolute difference (MAD) of 1.1 years (Pearson's $r = 0.762$, $p < 10^{-53}$; Table S2; median adult life expectancy in this population is 10.3 years for females and 7.94 for males [7]). Because the clock was significantly more accurate in males (N = 135; MAD = 0.9 years; Pearson's $r = 0.86$, $p < 10^{-40}$) than in females (N = 142; MAD = 1.6 years; $r = 0.78$, $p < 10^{-29}$; two-sided Wilcoxon test for differences in absolute error by sex: $p = 4.35 \times 10^{-9}$), we separated males and females for all subsequent analyses (Figure 1A and 1B).

Overall, the clock performed favorably relative to other morphological or biomarker predictors of age in this population. The epigenetic clock generally explained more variance in true chronological age, resulted in lower median error, and exhibited less bias than predictions based on body mass index (BMI) or blood cell composition data from flow cytometry or blood smears (traits found to change with age in baboons [8, 9]). Its performance was comparable to molar dentine exposure, a classical marker of age [10] (Figure S2). For 16 males and 14 females, we had two samples collected at different points in time. The predicted ages from these longitudinally collected samples were older for the later-collected samples, as expected (Figure 1C-D; binomial test $p = 5.95 \times 10^{-5}$). Furthermore, the change in epigenetic clock predictions between successive longitudinal samples positively predicted the actual change in age between sample dates ($\beta = 0.312$, $p = 0.027$).

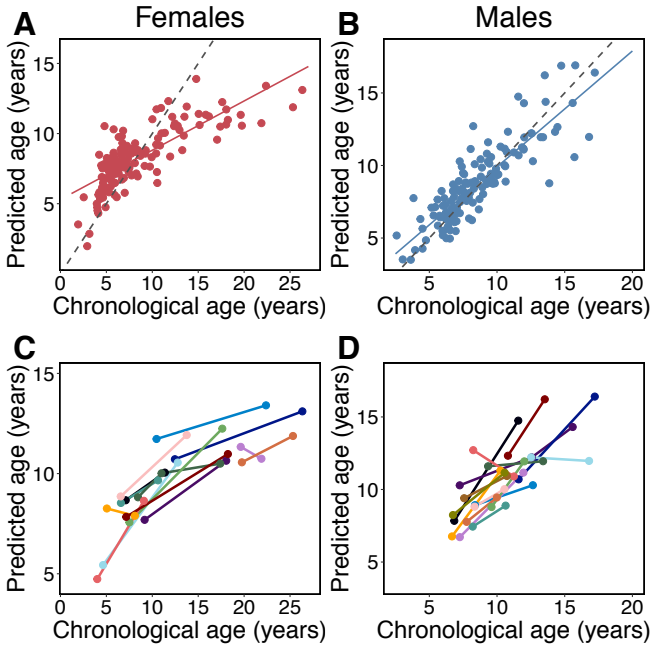

Figure 1. Epigenetic clock age predictions in the Amboseli baboons. Predicted ages are shown relative to true chronological ages for **(A)** females (Pearson's $r = 0.78$, $p < 10^{-29}$, N = 142 samples) and **(B)** males ($r = 0.86$, $p < 10^{-40}$, N = 135 samples). Solid lines represent the best fit line; dashed lines show the line for y = x. **(C)**

and **(D)** show predictions for individuals with at least two samples in the data set (14 females and 16 males, respectively). In 26 of 30 cases (87%), samples collected later were correctly predicted to be from an older animal.

In addition to differences in overall accuracy, sex differences were also apparent in the slope of the relationship between predicted age and chronological age. Males show a 2.2-fold higher rate of change in predicted age, as a function of chronological age, compared to females (Figure 1A-B; chronological age by sex interaction in a linear model for predicted age: $\beta = 0.448$, $p < 10^{-18}$, N = 277). This result agrees with previous findings showing that male baboons senesce more rapidly than females—a pattern shared with most other primates investigated thus far, including humans [11]. Interestingly, sex differences are not apparent in animals < 8 years, which roughly corresponds to the age at which the majority of males have achieved adult dominance rank and dispersed from their natal group [12-14] (N = 158, chronological age by sex interaction $\beta = -0.038$, $p = 0.808$). Rather, sex difference becomes apparent after baboons have reached full physiological and social adulthood (N = 119, chronological age by sex interaction $\beta = 0.459$, $p < 10^{-6}$ in animals ≥ 8 years), when divergence between male and female life history strategies is most marked [12-14] and when aging rates between the sexes are predicted to diverge [15-17]. This pattern suggests that within each sex, deviations between predicted age and chronological age—commonly interpreted as a measure of "biological age" or accelerated aging—may also be affected by environmental or life history variation, as has been suggested in humans, lab mice, and captive rhesus macaques [3, 4, 18, 19].

To test this hypothesis, we focused on four factors of known importance to fertility and/or survival components of fitness in the Amboseli baboon population. First, we investigated the effects of cumulative early adversity, which is a strong predictor of shortened lifespan in female baboons: females who experience three or more major sources of early adversity have expected adult lifespans that are a decade shorter than those who experience none [20]. Additionally, those females are less capable of raising their own juvenile offspring later in life, suggesting that early adversity compromises their physical condition over the long-term [21]. Following [20, 21], we measured cumulative adversity as a count of major adverse experiences suffered in early life, including low maternal social status, early life drought, a competing younger sibling, maternal loss, and high experienced population density. To maximize our sample size, we omitted early life social connectedness (included in [20] but omitted for the same reason in [21]), because social connectedness data were missing for mothers born relatively early in the long-term study. We predicted that high cumulative early adversity, which is linked to reduced lifespan, would predict increased biological age.

Second, we considered social bond strength in adulthood, which is positively associated with longer adult lifespan in female Amboseli baboons, human populations, and several other wild social mammals [22-24]. We predicted that low social bond strength, due to its relationship with decreased lifespan, would be associated with increased biological age.

Third, we investigated the effects of dominance rank, which is a major determinant of resource access in baboons. High-ranking males sire the most offspring, and high-ranking females experience shorter interbirth intervals, retain higher fertility during droughts, and form stronger social bonds with males [22, 25-27].

Finally, we assessed the effect of BMI, which captures dimensions of both body condition and competitive advantage [8]. In this case, we calculated BMI relative to the expected value for each male's age, which eliminates the correlation between BMI and age and BMI and rank. The predictions for dominance rank and body mass index associations were less clear: improved resource access could conceivably slow biological aging, but increased investment in growth and reproduction (either through higher fertility in females or physical competition for rank in males) could also be energetically costly.

We tested these predictions by modeling the deviation between predicted age and known chronological age (Δ_{age}) as a function of cumulative early adversity, ordinal dominance rank, body mass index (controlling for age), and for females, social bond strength to other females. Social bond strength was not included in the model for males, as this measure was unavailable for a large proportion of males in this data set (53.8%). We also included chronological age as a predictor in the model, as epigenetic age tends to be systematically overpredicted for young individuals and underpredicted for old individuals (Figure 1A-B); including chronological age in the model controls for this compression effect. No predictor variables were strongly linearly correlated (all $R^2 < 0.10$; Table S3).

Surprisingly, despite being two of the strongest known predictors of lifespan in wild baboons, neither cumulative early life adversity nor social bond strength explain variation in Δ_{age} (Table 1). In contrast, high male dominance rank is strongly and significantly associated with larger values of Δ_{age} ($\beta = -0.785$, $p = 7.0 \times 10^{-4}$; Figure 2; Table 1). Alpha males are predicted to be an average of 10.95 months older than their true chronological age—a difference that translates to 11.5% of a male baboon's expected adult lifespan [7].

Dominance rank is strongly age structured in male baboons: males tend to attain their highest rank between 7 and 12 years of age and fall in rank thereafter. Thus, nearly all males in the top four rank positions in our data set were between 7 and 12 years of age at the time they were sampled (however, because not all 7 – 12 year-olds are high-ranking, low rank positions include males of all age groups; Table S1, Figure S3). Our finding that high rank predicts accelerated epigenetic aging therefore implies that males incur the costs of high rank primarily in early to mid-adulthood, and only if they succeed in attaining high rank. Accelerated epigenetic aging is thus a function of absolute rank values, regardless of age, not deviations from the mean rank expected given a male's age (i.e., "rank-for-age," which can be quantified as the residuals of male dominance rank modeled as a quadratic function of chronological age: Figure S3). In support of this interpretation, a model that includes rank-for-age as an additional covariate recapitulates the significant effect of ordinal male rank ($p=0.045$), but finds no effect of rank-for-age ($p=0.819$; Table S4). In contrast, we observed no evidence for rank effects on Δ_{age} in females, consistent with overall sex differences in patterns of aging in primates and other mammals [15] and marked sex differences in the effects of rank on other molecular phenotypes in the Amboseli baboons specifically [11, 28].

Table 1. Predictors of Δ_{age}[1]				
Covariate	β (Female)	P-value (Female)	β (Male)	P-value (Male)
Intercept	**5.400**	**1.33×10^{-15}**	**3.294**	**1.19×10^{-8}**
Cumulative early adversity	-0.050	0.807	-0.005	0.973
Social bond strength	0.382	0.164	—	—
Dominance rank	0.025	0.228	**-0.078**	**7.39×10^{-4}**
Body mass index (age-adjusted)	0.026	0.682	**0.111**	**6.33×10^{-3}**
Chronological age	**-0.699**	**1.62×10^{-28}**	**-0.277**	**8.36×10^{-8}**

[1]Separate linear models for Δ_{age} were fit for females (N = 66) and for males (N = 93) for whom no data values were missing; social bond strength was not included in the model for males. Significant results are shown in bold.

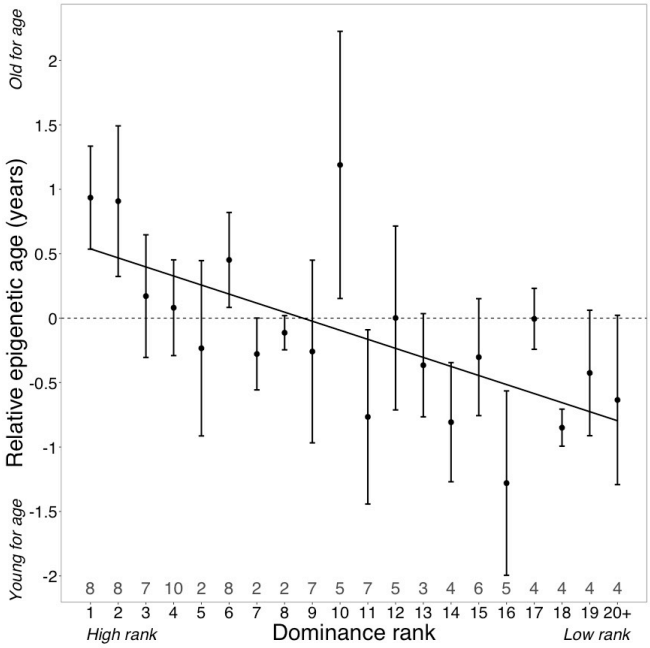

Figure 2. Dominance rank predicts epigenetic aging in male baboons. High rank is associated with elevated values of Δ_{age} (β = -0.0785, p = 7.39×10^{-4}, N = 105). The y-axis shows relative epigenetic age, a measure of epigenetic aging similar to Δ_{age} that is based on the sample-specific residuals from the relationship between predicted age and true chronological age. Positive (negative) values correspond to predicted ages that are older (younger) than expected for that chronological age. Dominance rank is measured using ordinal values, such that smaller values indicate higher rank. Dots and error bars represent the means and standard errors, respectively. Gray values above the x-axis indicate sample sizes for each rank.

Previous work has shown that high-ranking male baboons, but not high-ranking female baboons, up-regulate gene expression in inflammation-related and immune response pathways [28]. Elevated or chronic inflammation is thought to be one of the hallmarks of aging, and, in human populations, is one of the strongest predictors of mortality risk [29-31]. Consistent with these observations, CpG sites in the epigenetic clock that increase in DNA methylation with age (N = 459 sites) are enriched in or near genes that are up-regulated in the Amboseli baboons in response to the bacterial endotoxin lipopolysaccharide (LPS), which is a strong driver of inflammation (Figure S3; Fisher's exact test: $\log_2$(odds ratio) = 1.88, p = 0.001; gene expression data from [28]). In contrast, clock sites that decrease in DNA methylation with age (N = 134) are significantly enriched in or near genes that are down-regulated after LPS exposure (Fisher's exact test: $\log_2$(OR) =

184 3.28, $p = 0.002$). Clock sites, especially those for which DNA methylation is positively
185 correlated with age, are also enriched in genes, CpG islands, promoter regions, and putative
186 enhancers, compared to the background set of sites we initially considered as candidates
187 for inclusion in the clock (Figure S4; Fisher's exact tests, all $p < 0.005$; similar functional
188 enrichment has been found in a human epigenetic clock [2]). Moreover, clock sites are
189 enriched in regions previously found to change in methylation levels with age [32] and in
190 regions showing regulatory activity in high-throughput reporter assays [33]. Together,
191 these results suggest that accelerated epigenetic aging in males reflects functionally
192 important changes in DNA methylation levels, concentrated in immune response and
193 inflammation-related pathways.
194 In baboon males, dominance rank reflects physical condition and fighting ability.
195 Rank is therefore dynamic across the life course, such that males in their prime (ages 7 –
196 12) are most likely to be high-ranking, and the same male is likely to occupy multiple
197 positions in the social hierarchy during his lifetime [14]. If accelerations in epigenetic age
198 are tightly coupled to rank, our results predict that across longitudinally collected samples,
199 a male who becomes higher ranking should look older for age in his second sample relative
200 to first, whereas a male who loses status should look younger for age in his second sample
201 relative to first. To assess this possibility, we calculated the residuals of the best fit line
202 relating chronological age and predicted age ("relative epigenetic age") for 14 males for
203 whom we had repeated samples collected when they occupied different dominance rank
204 positions (N = 28 samples, 2 per male). In this data set, the sample collected when males
205 were higher status typically predicted higher values of relative epigenetic age compared to
206 the sample collected when they were lower status, consistent with high rank-associated
207 accelerated biological aging (Figure 3; paired t-test, $t = -2.31$, $p = 0.038$). For example, in the
208 case of one young adult male who we sampled at rank 18 and then rank 1, as he was first
209 climbing the social hierarchy, the actual time that elapsed between samples was 0.79 years
210 but he exhibited an increase in *predicted* age of 2.6 years. Moreover, the two males that
211 showed a decrease in predicted age, despite increasing in chronological age (Figure 1D),
212 were among those that experienced the greatest drop in social status between samples.
213 Thus, change in rank between samples for the same male predicted change in Δ_{age},
214 controlling for chronological age ($R^2 = 0.24$, $p=0.044$). Consistent with our cross-sectional
215 results, we did not observe evidence for a relationship between change in Δ_{age} and rank-
216 for-age ($R^2 = 0.14$, $p = 0.135$).

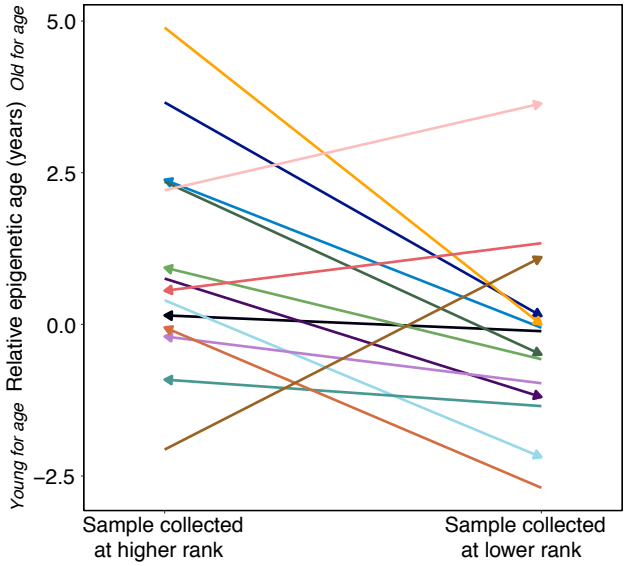

Figure 3. Male baboons exhibit higher relative epigenetic age when they occupy higher ranks. Relative epigenetic age for males in which multiple samples were collected when they occupied different ordinal rank values. Arrow indicates the temporal direction of rank changes: left-facing arrows represent cases in which the later sample was collected when males were higher-ranking, and right-facing arrows represent cases in the later sample was collected when males were lower-ranking.

Together, our findings indicate that major environmental predictors of lifespan and mortality risk (e.g., social bond strength and early life adversity in this population) do not necessarily predict epigenetic measures of biological age. Although this assumption is widespread in the literature, including for epigenetic clock analyses [34, 35], our results are broadly consistent with empirical results in humans. Specifically, while studies of early life adversity, which also predicts lifespan in human populations, find relatively consistent support for a relationship between early adversity and accelerated epigenetic aging in children and adolescents [36-41], there is little evidence for the long-term effects of early adversity on epigenetic age in adulthood [42-47]. Thus, while DNA methylation may make an important contribution to the biological embedding of early adversity into adulthood [48, 49], it does not seem to do so through affecting the epigenetic clock itself. Social and environmental effects on the clock instead seem to be most influenced by concurrent conditions, lending support to "recency" models for environmental effects on aging that posit that health is more affected by the current environment than past experience [50-52]. Additional longitudinal sampling will be necessary to evaluate whether current conditions alone can explain accelerated epigenetic aging, or whether it also requires integrating the effects of exposures across the life course (the "accumulation" model: [50, 52]). Repeated samples could also help exclude an alternative explanation for our findings: that viability selection against individuals who experienced high early adversity attenuates the true effect of cumulative early adversity on relative epigenetic age.

Finally, our analyses reveal that males who achieve high rank appear epigenetically older than expected given their known chronological age. Although high ranking males also tend to be larger due to increased muscle mass (Pearson's r between rank and BMI = 0.56, $p = 6.38 \times 10^{-9}$), we observed an additional, independent effect of age-adjusted BMI: males who had high BMI relative to their age also looked older for age, controlling for rank and age ($\beta = 0.1107$, $p = 0.006$) (Table 1). These two effects suggest that investment in body

condition, which is a crucial factor in male competitive ability, incurs other physiological costs that compound to influence biological age. Indeed, previous research on the Amboseli baboons also points to costs of high rank, including high levels of glucocorticoids in alpha males [53], increased expression of genes involved in innate immunity and inflammation [28], and a trend towards elevated mortality risk [54]. These associations may arise because high-ranking males are both more likely to engage in physical conflict with other males, and more likely to spend long periods of time in energetically costly mate-guarding [55, 56]. Alternatively, males who are able to make significant investments in body condition, while tolerating their accompanying costs, may be able to successfully maintain high rank. Importantly, since doing so is likely to contribute to higher lifetime reproductive success for male baboons, the fitness-associated benefits of high rank can exceed the costs, even if accelerated biological aging increases the risk of mortality.

Acknowledgements

We gratefully acknowledge the support provided by the National Science Foundation and the National Institutes of Health for the majority of the data represented here, currently through NSF IOS 1456832, NIH R01AG053308, R01AG053330, R01HD088558, and P01AG031719. R.A.J. is supported by NIH F32HD095616 and J.A.A. by NSF #2018264636. We thank the members of the Amboseli Baboon Research Project for collecting the data presented here, especially J. Altmann for her foundational role in establishing the study population and these data sets; J. Gordon, N. Learn, and K. Pinc for managing the database; R.S. Mututua, S. Sayialel, and J.K. Warutere for data collection in the field; and T. Wango and V. Oudu for their assistance in Nairobi. We also thank the Kenya Wildlife Service, University of Nairobi, the Institute of Primate Research, the National Museums of Kenya, the National Council for Science, Technology, and Innovation, members of the Amboseli-Longido pastoralist communities, the Enduimet Wildlife Management Area, Ker & Downey Safaris, Air Kenya, and Safarilink for their assistance in Kenya. Finally, we thank current and past members of the Tung, Alberts, Archie, and Altmann labs for their helpful feedback. This research was approved by IACUCs at Duke University, University of Notre Dame, and Princeton University and adhered to all the laws and guidelines of Kenya. For a complete set of acknowledgments of funding sources, logistical assistance, and data collection and management, please visit http://amboselibaboons.nd.edu/acknowledgements/.

Author Contributions

Conceptualization, R.A.J., J.A.A., J.T., E.A.A., A.J.L.; Investigation, J.A.A., R.A.J., A.J.L., F.A.C., M.Y.A., T.N.V., and J.T.; Formal Analysis, J.A.A. and R.A.J.; Writing—Original Draft, R.A.J., J.A.A., and J.T.; Writing—Reviewing & Editing, R.A.J., J.A.A., A.J.L., T.N.V., M.Y.A., F.A.C., S.C.A., E.A.A., and J.T. Funding Acquisition, J.T., S.C.A., and E.A.A. Supervision, J.T.

Declaration of Interests

The authors declare no competing interests.

STAR Methods

Study population and biological sample collection

This study focused on a longitudinally monitored population of wild baboons (*Papio cynocephalus*, the yellow baboon, with some admixture from the closely related anubis baboon *P. anubis* [57, 58]) in the Amboseli ecosystem of Kenya. This population has been continuously monitored by the Amboseli Baboon Research Project (ABRP) since 1971 [6]. For the majority of study subjects (N = 242 of 245 individuals), birth dates were therefore known to within a few days' error; for the remainder, birth dates were known within 3 months' error (Table S1).

All DNA methylation data were generated from blood-derived DNA obtained during periodic darting efforts, as detailed in [28, 59, 60]. Samples were obtained under approval from the Institutional Animal Care and Use Committee (IACUC) of Duke University and adhered to all the laws and guidelines of Kenya. In brief, individually recognized study subjects were temporarily anesthetized using a Telazol-loaded dart delivered through a blow gun. Baboons were then safely moved to a new location where blood samples and morphometric data, including body mass and crown-rump length, were collected. Baboons were then allowed to recover from anesthesia in a covered holding cage and released to their group within 2 – 4 hours. Blood samples were stored at -20 C in Kenya until export to the United States.

DNA methylation data

DNA methylation data were generated from blood-extracted DNA collected from known individuals in the Amboseli study population (N = 277 samples from 245 animals; 14 females and 14 males were each sampled twice, and 1 female and 1 male were each sampled three times). Here, we analyzed a combined data set that included previously published reduced representation bisulfite sequencing [61] (RRBS) data from the same population (N = 36) [5] and new RRBS data from 241 additional individuals.

RRBS libraries were constructed following [62], using ~200 ng baboon DNA plus 0.2 ng unmethylated lambda phage DNA per sample as input. Samples were sequenced to a mean depth of 17.8 (± 10.5 s.d.) million reads on either the Illumina HiSeq 2000 or HiSeq 4000 platform (Table S1), with an estimated mean bisulfite conversion efficiency (based on the conversion rate of lambda phage DNA) of 99.8% (minimum = 98.1%). Sequence reads were trimmed with Trim Galore! [63] to remove adapters and low quality sequence (Phred score < 20). Trimmed reads were mapped with BSMAP [64] to the baboon genome (*Panu2.0*) allowing a 10% mismatch rate to account for the degenerate composition of bisulfite-converted DNA. We used the mapped reads to count the number of methylated and total reads per CpG site, per sample [64, 65]. Following [5, 32], CpG sites were filtered to retain sites with a mean methylation level between 0.1 and 0.9 (i.e., to exclude constitutively hyper- or hypo-methylated sites) and mean coverage ≥5x. We also excluded any CpG sites with missing data for ≥15% of individuals in the sample. After filtering, we retained N = 458,504 CpG sites for downstream analysis. For the remaining missing data (mean number of missing sites per sample = 1.4% ± 3.5% s.d., equivalent to 6,409 ± 16,024 sites), we imputed methylation levels using a k-nearest neighbors approach in the R package *impute*, using default parameters [66].

337 *Building the epigenetic clock*
338 We used the R package *glmnet* [67] to build a DNA methylation clock for baboons.
339 Specifically, we fit a linear model in which the predictor variables were normalized levels of
340 DNA methylation at 458,504 candidate clock CpG sites across the genome and the response
341 variable was chronological age. To account for the excess of CpG sites relative to samples,
342 *glmnet* uses an elastic net penalty to shrink predictor coefficients toward 0 [68]. Optimal
343 alpha parameters were identified by grid searching across a range of alphas from 0
344 (equivalent to ridge regression) to 1 (equivalent to LASSO) by increments of 0.1. We
345 defined the optimal alpha as the value that maximized R^2 between predicted and true
346 chronological age across all samples. We set the regularization parameter lambda to the
347 value that minimized mean-squared error during n-fold internal cross-validation.
348 To generate predicted age estimates for a given sample, we used a leave-one-out
349 cross-validation approach in which all samples but the "test" sample were included for
350 model training, and the resulting model was used to predict age for the left-out test sample.
351 Importantly, training samples were scaled independently of the test sample in each leave-
352 one-out model to avoid bleed-through of information from the test data into the training
353 data. To do so, we first quantile normalized methylation ratios (the proportion of
354 methylated counts to total counts for each CpG site) within each sample to a standard
355 normal distribution. Training samples were then separated from the test sample and the
356 methylation levels for each CpG site in the training set were quantile normalized across
357 samples to a standard normal distribution. For predicting age in the test sample, we
358 compared the methylation value for each site in the test sample to the empirical cumulative
359 distribution function for the training samples (at the same site) to estimate the quantile in
360 which the training sample methylation ratio fell. The training sample was then assigned the
361 same quantile value from the standard normal distribution using the function *qnorm* in R.
362
363 *Comparisons to alternative predictors of aging*
364 To assess the utility of the DNA methylation clock relative to other data types, we
365 compared its predictive accuracy to clocks based on three other age-related phenotypes:
366 tooth wear (percent molar dentine exposure [10]), body condition (body mass index: BMI
367 [8]), and blood cell type composition (blood smear counts and lymphocyte/monocyte
368 proportions from flow cytometry performed on peripheral blood mononuclear cells, as in
369 [28, 69]). Leave-one-out model training and prediction were performed for each data type
370 using linear modeling (i.e., not glmnet, since the number of features was much less than the
371 number of samples in this case). To compare the relative predictive accuracy of each data
372 type, we calculated the R^2 between predicted and chronological age, the median absolute
373 difference between predicted and chronological age, and the bias in age predictions (the
374 absolute value of 1- slope of the best fit line between predicted and chronological age)
375 (Figure S2).
376 *Tooth wear.* Molar enamel in baboons wears away with age to expose the underlying
377 dentine layer. Percent dentine exposure (PDE) on the molar occlusal surface has been
378 shown to be strongly age-correlated in previous work [10]. To assess its predictive power,
379 we obtained PDE data from tooth casts reported by Galbany and colleagues [10] for the left
380 upper molars (tooth positions M1, M2, M3) and left lower molars (tooth positions M1, M2,
381 M3) for 39 males and 34 females in our data set. For each molar position (M1, M2, M3)
382 within each individual, we calculated PDE as the mean for the upper and lower molars.

383 Because dentine exposure scales quadratically with respect to age [10], we fit age as a
384 function of PDE using the following model: $age \sim \sqrt{PDE_{M1}} + \sqrt{PDE_{M2}} + \sqrt{PDE_{M3}}$.
385 *Body mass index.* For both male and female baboons in Amboseli, body mass
386 increases with age until individuals reach peak size, and then tends to decrease with age as
387 animals lose fat and/or muscle mass [8]. To quantify body condition using body mass, we
388 calculated body mass index (BMI) values for 139 males and 154 females for whom body
389 mass and crown-rump length data were available from periodic darting efforts. We
390 retained only measures taken from animals born into and sampled in wild-feeding study
391 groups, when sex-skin swellings (in females only) that could affect crown-rump length
392 measures were absent. BMI was calculated as mass (kilograms) divided by crown-rump
393 length (meters squared), following [70]. To assess the predictive power of BMI for age, we
394 built sex-specific piecewise-regression models. Breakpoints for the piecewise-regression
395 models (to separate "youthful" versus "aged" animals) were set at 8 years old for males and
396 10 years old for females, following findings from previous work on body mass in the
397 Amboseli population [8].
398 *Blood cell type composition.* The proportions of different cell types in blood change
399 across the life course, including in baboons [9]. We assessed the predictive power of blood
400 cell composition for age using two data sets. First, we used data collected from blood smear
401 counts (N = 134) for five major white blood cell types: basophils, eosinophils, monocytes,
402 lymphocytes, and neutrophils. Second, we used data on the proportional representation of
403 five peripheral blood mononuclear cell (PBMC) subsets: cytotoxic T cells, helper T cells, B
404 cells, monocytes, and natural killer cells, measured using flow cytometry as reported by Lea
405 and colleagues [28] (N = 53). Cell types were included as individual covariates for leave-
406 one-out model training.
407
408 *Sources of variance in predicted age*
409 We asked whether factors known to be associated with inter-individual variation in
410 fertility or survival also predict inter-individual variation in Δ_{age} (predicted age from the
411 epigenetic clock minus known chronological age). To do so, we fit linear models separately
412 for males and females, with Δ_{age} as the dependent variable and dominance rank at the time
413 of sampling, cumulative early adversity, relative BMI (corrected for age), and chronological
414 age as predictor variables [20]). For females, we also included a measure of social bond
415 strength to other females as a predictor variable, based on findings that show that socially
416 isolated females experience higher mortality rates in adulthood [22, 71]. Samples with
417 missing values for any of the predictor variables were excluded in the model, resulting in a
418 final analysis set of 66 female samples (from 59 females) and 93 male samples (from 84
419 males). The chronological ages of samples with complete data relative to samples with
420 missing data were equivalent for females (t-test, t = 1.95, p = 0.053) but were slighly lower
421 for males (t-test, t = -3.04, p = 0.003; mean chronological ages are 7.98 and 9.65 years for
422 complete and missing samples, respectively). Predictor variables were measured as
423 follows.
424 *Dominance rank.* Sex-specific dominance hierarchies were constructed monthly for
425 every social group in the study population based on the outcomes of dyadic aggressive
426 encounters. Ordinal dominance ranks were assigned to every adult based on these
427 hierarchies, such that low numbers represent high rank/social status and high numbers

represent low rank/social status [72]. Although most analyses of data from the Amboseli baboons have used ordinal ranks as the primary measure of social status, in some analyses proportional rank (i.e., the proportion of same-sex members of an individual's social group that he or she dominates) has proven to be a stronger predictor of behavioral, life history, or physiological outcomes [73]. In this study, we chose to use ordinal ranks, but proportional and ordinal dominance rank were highly correlated in our dataset (r^2=.70, p=1.13 x 10^{-58}). Using proportional rank rather than ordinal rank did not qualitatively affect our analyses. Additionally, to investigate whether the patterns we observed are due to a consistent effect of rank across all ages, or instead an effect of being high or low rank relative to the expected (mean) value for a male's age, we also calculated a "rank-for-age" value. Rank-for-age is defined as the residuals of a model with dominance rank as the response variable and age and age^2 as the predictor variables (Fig S4).

Cumulative early adversity. Previous work in Amboseli defined a cumulative early adversity score as the sum of 6 different adverse conditions that a baboon could experience during early life [20]. This index strongly predicts adult lifespan in female baboons, and a modified version of this index also predicts offspring survival [21]. To maximize the sample size available for analysis, we excluded maternal social connectedness, the source of adversity with the highest frequency of missing data, leaving us with a cumulative early adversity score generated from 5 different binary-coded adverse experiences. These experiences were: (i) early life drought (defined as ≤ 200 mm of rainfall in the first year of life), which is linked to reduced fertility in females [27, 74]; (ii) having a low ranking mother (defined as falling within the lowest quartile of ranks for individuals in the dataset), which predicts rates of maturation [75-77]; (iii) having a close-in-age younger sibling (<1.5 years), which may redirect maternal investment to the sibling [78], (iv) being born into a large social group, which may increase within-group competition for shared resources [27, 77, 79], and (v) maternal death before the age of 4, which results in a loss of both social and nutritional resources [77, 80].

Body mass index. BMI was modeled as the residuals from sex-specific piecewise regression models relating BMI to age. By taking this approach, we asked whether having relatively high BMI for one's age and sex predicted higher (or lower) Δ_{age}.

Social bond strength. For this analysis, we measured female social bond strength to other females using the dyadic sociality index (F-DSI) [54]. We did not include this parameter (male's social bond strength to females) for the male model, because this measure is unavailable for young males in this dataset. F-DSI was calculated as an individual's average bond strength with her top three female social partners, in the 365 days prior to the day of sampling, controlling for observer effort. This approach is based on representative interaction sampling of grooming interactions between females, in which observers record all grooming interactions in their line of sight while moving through the group conducting random-ordered, 10-minute long focal animal samples of pre-selected individuals. Because smaller groups receive more observer effort per individual and per dyad (and thus record more grooming interactions per individual or dyad), we estimated observer effort for dyad *d* in year *y* as:

$$E_{d,y} = \frac{c_d(s_d)}{f_d}$$

where c_d is the number of days the two females in a dyad were coresident in the same

472 social group, s_d is the number of focal samples taken during the dyad's coresidence, and f_d
473 is the average number of females in the group during the dyad's coresidence.
474 F-DSI for each adult female dyad in each year is the z-scored residual, ε, from the
475 model:
476 $$\log(R_{d,y}) = \beta(\log(E_{d,y})) + \varepsilon$$
477 where $R_{d,y}$ is the number of grooming interactions for dyad d in year y divided by the
478 number of days that the two individuals were coresident, and $E_{d,y}$ is observer effort.
479
480 *Analysis of longitudinal samples*
481 To test whether changes in rank predict changes in relative epigenetic age within
482 individuals, we used data from 5 males from the original dataset and generated additional
483 RRBS data for 9 samples, resulting in a final set of 14 males who each were sampled at least
484 twice in the data set, when they occupied different ordinal ranks (mean years elapsed
485 between samples = 3.92 ± 1.94 s.d.; mean absolute difference in dominance ranks = 6.86 ±
486 5.07 s.d.). This effort increased our total sample size to N = 286 samples from 248 unique
487 individuals. To incorporate the new samples into our analysis, we reperformed leave-one-
488 out age prediction with N-fold internal cross validation at the optimal alpha selected for the
489 original N = 277 samples (alpha = 0.1). For the 277 samples carried over from the original
490 analysis, we verified that age predictions were nearly identical between the previous
491 analysis and the expanded data set ($R^2 = 0.98$, $p = 2.21 \times 10^{-239}$).
492 Based on the new age predictions for males in the data set (N = 144), we again
493 calculated relative epigenetic age as the residual of the best fit line relating predicted age to
494 chronological age. We then used the 14 males with repeated DNA methylation profiles and
495 rank measures in this dataset to test whether, within individuals, changes in dominance
496 rank or rank-for-age explained changes in relative epigenetic age between samples.
497
498 *Epigenetic clock enrichment analyses*
499 To evaluate whether CpG sites included in the epigenetic clock were enriched in
500 functionally important regions of the baboon genome [32, 81], we used two-sided Fisher's
501 exact tests to investigate enrichment/depletion of the 593 epigenetic clock sites in (i) gene
502 bodies and exons, based on the Ensembl annotation *Panu2.0.90*; (ii) CpG islands annotated
503 in the UCSC Genome Browser; (iii) CpG shores, defined as the 2,000 basepairs flanking CpG
504 islands (following [32, 81, 82]); and (iv) promoter regions, defined as the 2,000 basepairs
505 upstream of the 5'-most annotated transcription start site for each protein-coding gene
506 (following [32, 81]). We also considered (v) putative enhancer regions, which have not
507 been annotated for the *Panu2.0* assembly. We therefore used ENCODE H3K4me1 ChIP-seq
508 data from humans [83] and the *liftOver* tool to define likely enhancer coordinates in
509 *Panu2.0*.
510 We also tested for enrichment of clock sites in regions of the genome that have been
511 identified by previous empirical studies to be of special interest. First, we considered
512 regions that likely have regulatory activity in blood cells, defined as all 200 base-pair
513 windows that showed evidence of enhancer activity in a recently performed massively
514 parallel reporter assay [33]. We used *liftOver* to identify the inferred homologous *Panu2.0*
515 coordinates for these windows, which were originally defined in the human genome.
516 Second, we defined age-related differentially methylated regions (age DMRs) in the

517 Amboseli baboons based on genomic intervals found, in previous analyses, to contain at
518 least three closely spaced age-associated CpG sites (inter-CpG distance ≤ 1kb), as described
519 in [32]. Third, we defined lipopolysaccharide (LPS) up-regulated and LPS down-regulated
520 genes as those genes that were significantly differentially expressed (1% false discovery
521 rate) between unstimulated Amboseli baboon white blood cells and LPS-stimulated cells
522 from the same individual, following 10 hours of culture in parallel [28].
523
524 Data and code availabity
525 All sequencing data generated during this study are available in the NCBI Sequence Read
526 Archive (project accession PRJNA607996).

527 References

528 1. Hannum, G., Guinney, J., Zhao, L., Zhang, L., Hughes, G., Sadda, S., Klotzle, B., Bibikova,
529 M., Fan, J.-B., and Gao, Y. (2013). Genome-wide methylation profiles reveal
530 quantitative views of human aging rates. Molecular cell *49*, 359-367.
531 2. Horvath, S. (2013). DNA methylation age of human tissues and cell types. Genome
532 biology *14*, 3156.
533 3. Petkovich, D.A., Podolskiy, D.I., Lobanov, A.V., Lee, S.-G., Miller, R.A., and Gladyshev,
534 V.N. (2017). Using DNA methylation profiling to evaluate biological age and
535 longevity interventions. Cell metabolism *25*, 954-960. e956.
536 4. Stubbs, T.M., Bonder, M.J., Stark, A.-K., Krueger, F., von Meyenn, F., Stegle, O., and
537 Reik, W. (2017). Multi-tissue DNA methylation age predictor in mouse. Genome
538 biology *18*, 68.
539 5. Lea, A.J., Altmann, J., Alberts, S.C., and Tung, J. (2016). Resource base influences
540 genome‐wide DNA methylation levels in wild baboons (Papio cynocephalus).
541 Molecular ecology *25*, 1681-1696.
542 6. Alberts, S.C., and Altmann, J. (2012). The Amboseli Baboon Research Project: 40
543 years of continuity and change. In Long-term field studies of primates. (Springer),
544 pp. 261-287.
545 7. Colchero, F., Rau, R., Jones, O.R., Barthold, J.A., Conde, D.A., Lenart, A., Nemeth, L.,
546 Scheuerlein, A., Schoeley, J., and Torres, C. (2016). The emergence of longevous
547 populations. Proceedings of the National Academy of Sciences *113*, E7681-E7690.
548 8. Altmann, J., Gesquiere, L., Galbany, J., Onyango, P.O., and Alberts, S.C. (2010). Life
549 history context of reproductive aging in a wild primate model. Annals of the New
550 York Academy of Sciences *1204*, 127-138.
551 9. Jayashankar, L., Brasky, K.M., Ward, J.A., and Attanasio, R. (2003). Lymphocyte
552 modulation in a baboon model of immunosenescence. Clin. Diagn. Lab. Immunol. *10*,
553 870-875.
554 10. Galbany, J., Altmann, J., Pérez‐Pérez, A., and Alberts, S.C. (2011). Age and individual
555 foraging behavior predict tooth wear in Amboseli baboons. American Journal of
556 Physical Anthropology *144*, 51-59.
557 11. Bronikowski, A.M., Altmann, J., Brockman, D.K., Cords, M., Fedigan, L.M., Pusey, A.,
558 Stoinski, T., Morris, W.F., Strier, K.B., and Alberts, S.C. (2011). Aging in the natural
559 world: comparative data reveal similar mortality patterns across primates. Science
560 *331*, 1325-1328.
561 12. Alberts, S.C., and Altmann, J. (1995). Balancing costs and opportunities: dispersal in
562 male baboons. The American Naturalist *145*, 279-306.
563 13. Alberts, S.C., and Altmann, J. (1995). Preparation and activation: determinants of age
564 at reproductive maturity in male baboons. Behavioral Ecology and Sociobiology *36*,
565 397-406.
566 14. Alberts, S.C., Watts, H.E., and Altmann, J. (2003). Queuing and queue-jumping: long-
567 term patterns of reproductive skew in male savannah baboons, Papio cynocephalus.
568 Animal Behaviour *65*, 821-840.
569 15. Clutton-Brock, T.H., and Isvaran, K. (2007). Sex differences in ageing in natural
570 populations of vertebrates. Proceedings of the Royal Society B: Biological Sciences
571 *274*, 3097-3104.

572 16. Kirkwood, T.B., and Rose, M.R. (1991). Evolution of senescence: late survival
573 sacrificed for reproduction. Philosophical Transactions of the Royal Society of
574 London. Series B: Biological Sciences *332*, 15-24.
575 17. Williams, G.C. (1957). Pleiotropy, natural selection, and the evolution of senescence.
576 evolution, 398-411.
577 18. Maegawa, S., Lu, Y., Tahara, T., Lee, J.T., Madzo, J., Liang, S., Jelinek, J., Colman, R.J.,
578 and Issa, J.-P.J. (2017). Caloric restriction delays age-related methylation drift.
579 Nature communications *8*, 539.
580 19. Ryan, J., Wrigglesworth, J., Loong, J., Fransquet, P.D., and Woods, R.L. (2019). A
581 systematic review and meta-analysis of environmental, lifestyle and health factors
582 associated with DNA methylation age. The journals of gerontology. Series A,
583 Biological sciences and medical sciences.
584 20. Tung, J., Archie, E.A., Altmann, J., and Alberts, S.C. (2016). Cumulative early life
585 adversity predicts longevity in wild baboons. Nature communications *7*, 11181.
586 21. Zipple, M.N., Archie, E.A., Tung, J., Altmann, J., and Alberts, S.C. (2019).
587 Intergenerational effects of early adversity on survival in wild baboons. eLife *8*,
588 e47433.
589 22. Archie, E.A., Tung, J., Clark, M., Altmann, J., and Alberts, S.C. (2014). Social affiliation
590 matters: both same-sex and opposite-sex relationships predict survival in wild
591 female baboons. Proceedings of the Royal Society B: Biological Sciences *281*,
592 20141261.
593 23. Holt-Lunstad, J., Smith, T.B., and Layton, J.B. (2010). Social relationships and
594 mortality risk: a meta-analytic review. PLoS Med *7*, e1000316.
595 24. Snyder-Mackler, N., Burger, J.R., Gaydosh, L., Belsky, D., Noppert, G.A., Campos, F.A.,
596 Bartolomucci, A., Yang, Y.C., Aiello, A.E., O'Rand, A., et al. Social determinants of
597 health and survival in humans and other animals. In review.
598 25. Alberts, S.C., Buchan, J.C., and Altmann, J. (2006). Sexual selection in wild baboons:
599 from mating opportunities to paternity success. Animal Behaviour *72*, 1177-1196.
600 26. Gesquiere, L.R., Altmann, J., Archie, E.A., and Alberts, S.C. (2018). Interbirth intervals
601 in wild baboons: Environmental predictors and hormonal correlates. American
602 journal of physical anthropology *166*, 107-126.
603 27. Lea, A.J., Altmann, J., Alberts, S.C., and Tung, J. (2015). Developmental constraints in
604 a wild primate. The American Naturalist *185*, 809-821.
605 28. Lea, A.J., Akinyi, M.Y., Nyakundi, R., Mareri, P., Nyundo, F., Kariuki, T., Alberts, S.C.,
606 Archie, E.A., and Tung, J. (2018). Dominance rank-associated gene expression is
607 widespread, sex-specific, and a precursor to high social status in wild male baboons.
608 Proceedings of the National Academy of Sciences *115*, E12163-E12171.
609 29. Castagné, R., Garès, V., Karimi, M., Chadeau-Hyam, M., Vineis, P., Delpierre, C., Kelly-
610 Irving, M., and Consortium, L. (2018). Allostatic load and subsequent all-cause
611 mortality: which biological markers drive the relationship? Findings from a UK birth
612 cohort. European journal of epidemiology *33*, 441-458.
613 30. Levine, M.E. (2012). Modeling the rate of senescence: can estimated biological age
614 predict mortality more accurately than chronological age? Journals of Gerontology
615 Series A: Biomedical Sciences and Medical Sciences *68*, 667-674.
616 31. López-Otín, C., Blasco, M.A., Partridge, L., Serrano, M., and Kroemer, G. (2013). The
617 hallmarks of aging. Cell *153*, 1194-1217.

618 32. Lea, A.J., Tung, J., and Zhou, X. (2015). A flexible, efficient binomial mixed model for
619 identifying differential DNA methylation in bisulfite sequencing data. PLoS genetics
620 *11*, e1005650.
621 33. Lea, A.J., Vockley, C.M., Johnston, R.A., Del Carpio, C.A., Barreiro, L.B., Reddy, T.E., and
622 Tung, J. (2018). Genome-wide quantification of the effects of DNA methylation on
623 human gene regulation. eLife *7*, e37513.
624 34. Liu, Z., Chen, B.H., Assimes, T.L., Ferrucci, L., Horvath, S., and Levine, M.E. (2019). The
625 role of epigenetic aging in education and racial/ethnic mortality disparities among
626 older US Women. Psychoneuroendocrinology *104*, 18-24.
627 35. Shalev, I., and Belsky, J. (2016). Early-life stress and reproductive cost: A two-hit
628 developmental model of accelerated aging? Medical Hypotheses *90*, 41-47.
629 36. Brody, G.H., Miller, G.E., Yu, T., Beach, S.R., and Chen, E. (2016). Supportive family
630 environments ameliorate the link between racial discrimination and epigenetic
631 aging: A replication across two longitudinal cohorts. Psychological Science *27*, 530-
632 541.
633 37. Brody, G.H., Yu, T., Chen, E., Beach, S.R., and Miller, G.E. (2016). Family‐centered
634 prevention ameliorates the longitudinal association between risky family processes
635 and epigenetic aging. Journal of child psychology and psychiatry *57*, 566-574.
636 38. Davis, E., Humphreys, K., McEwen, L., Sacchet, M., Camacho, M., MacIsaac, J., Lin, D.,
637 Kobor, M., and Gotlib, I. (2017). Accelerated DNA methylation age in adolescent
638 girls: associations with elevated diurnal cortisol and reduced hippocampal volume.
639 Translational psychiatry *7*, e1223.
640 39. Jovanovic, T., Vance, L.A., Cross, D., Knight, A.K., Kilaru, V., Michopoulos, V., Klengel,
641 T., and Smith, A.K. (2017). Exposure to violence accelerates epigenetic aging in
642 children. Scientific reports *7*, 8962.
643 40. Marini, S., Davis, K.A., Soare, T.W., Suderman, M.J., Simpkin, A.J., Smith, A.D., Wolf, E.J.,
644 Relton, C.L., and Dunn, E.C. (2018). Predicting cellular aging following exposure to
645 adversity: Does accumulation, recency, or developmental timing of exposure
646 matter? BioRxiv, 355743.
647 41. Sumner, J.A., Colich, N.L., Uddin, M., Armstrong, D., and McLaughlin, K.A. (2019).
648 Early experiences of threat, but not deprivation, are associated with accelerated
649 biological aging in children and adolescents. Biological psychiatry *85*, 268-278.
650 42. Austin, M.K., Chen, E., Ross, K.M., McEwen, L.M., MacIsaac, J.L., Kobor, M.S., and
651 Miller, G.E. (2018). Early-life socioeconomic disadvantage, not current, predicts
652 accelerated epigenetic aging of monocytes. Psychoneuroendocrinology *97*, 131-134.
653 43. Boks, M.P., van Mierlo, H.C., Rutten, B.P., Radstake, T.R., De Witte, L., Geuze, E.,
654 Horvath, S., Schalkwyk, L.C., Vinkers, C.H., and Broen, J.C. (2015). Longitudinal
655 changes of telomere length and epigenetic age related to traumatic stress and post-
656 traumatic stress disorder. Psychoneuroendocrinology *51*, 506-512.
657 44. Lawn, R.B., Anderson, E.L., Suderman, M., Simpkin, A.J., Gaunt, T.R., Teschendorff,
658 A.E., Widschwendter, M., Hardy, R., Kuh, D., and Relton, C.L. (2018). Psychosocial
659 adversity and socioeconomic position during childhood and epigenetic age: analysis
660 of two prospective cohort studies. Human molecular genetics *27*, 1301-1308.
661 45. Simons, R.L., Lei, M.K., Beach, S.R., Philibert, R.A., Cutrona, C.E., Gibbons, F.X., and
662 Barr, A. (2016). Economic hardship and biological weathering: the epigenetics of

aging in a US sample of black women. Social Science & Medicine *150*, 192-200.
46. Wolf, E.J., Maniates, H., Nugent, N., Maihofer, A.X., Armstrong, D., Ratanatharathorn, A., Ashley-Koch, A.E., Garrett, M., Kimbrel, N.A., and Lori, A. (2018). Traumatic stress and accelerated DNA methylation age: a meta-analysis. Psychoneuroendocrinology *92*, 123-134.
47. Zannas, A.S., Arloth, J., Carrillo-Roa, T., Iurato, S., Röh, S., Ressler, K.J., Nemeroff, C.B., Smith, A.K., Bradley, B., and Heim, C. (2015). Lifetime stress accelerates epigenetic aging in an urban, African American cohort: relevance of glucocorticoid signaling. Genome biology *16*, 266.
48. Aristizabal, M.J., Anreiter, I., Halldorsdottir, T., Odgers, C.L., McDade, T.W., Goldenberg, A., Mostafavi, S., Kobor, M.S., Binder, E.B., and Sokolowski, M.B. (2019). Biological embedding of experience: A primer on epigenetics. Proceedings of the National Academy of Sciences, 201820838.
49. Hertzman, C. (2012). Putting the concept of biological embedding in historical perspective. Proceedings of the National Academy of Sciences *109*, 17160-17167.
50. Ben-Shlomo, Y., and Kuh, D. (2002). A life course approach to chronic disease epidemiology: conceptual models, empirical challenges and interdisciplinary perspectives. (Oxford University Press).
51. Shanahan, L., Copeland, W.E., Costello, E.J., and Angold, A. (2011). Child-, adolescent- and young adult-onset depressions: differential risk factors in development? Psychological medicine *41*, 2265-2274.
52. Shanahan, M.J., and Hofer, S.M. (2011). Molecular genetics, aging, and well-being: Sensitive period, accumulation, and pathway models. In Handbook of aging and the social sciences. (Elsevier), pp. 135-147.
53. Gesquiere, L.R., Learn, N.H., Simao, M.C.M., Onyango, P.O., Alberts, S.C., and Altmann, J. (2011). Life at the top: rank and stress in wild male baboons. Science *333*, 357-360.
54. Campos, F.A., Villavicencio, F., Archie, E.A., Colchero, F., and Alberts, S.C. (2020). Social relationships, social status, and survival in wild baboons: A tale of two sexes. Philosophical Transactions of the Royal Society. Series B: Biological Sciences.
55. Archie, E.A., Altmann, J., and Alberts, S.C. (2012). Social status predicts wound healing in wild baboons. Proceedings of the National Academy of Sciences *109*, 9017-9022.
56. Rasmussen, K. (1985). Changes in the activity budgets of yellow baboons (Papio cynocephalus) during sexual consortships. Behavioral Ecology and Sociobiology *17*, 161-170.
57. Alberts, S.C., and Altmann, J. (2001). Immigration and hybridization patterns of yellow and anubis baboons in and around Amboseli, Kenya. American Journal of Primatology: Official Journal of the American Society of Primatologists *53*, 139-154.
58. Tung, J., Charpentier, M.J., Garfield, D.A., Altmann, J., and Alberts, S.C. (2008). Genetic evidence reveals temporal change in hybridization patterns in a wild baboon population. Molecular Ecology *17*, 1998-2011.
59. Altmann, J., Alberts, S.C., Haines, S.A., Dubach, J., Muruthi, P., Coote, T., Geffen, E., Cheesman, D.J., Mututua, R.S., and Saiyalel, S.N. (1996). Behavior predicts genes structure in a wild primate group. Proceedings of the National Academy of Sciences *93*, 5797-5801.

60. Tung, J., Zhou, X., Alberts, S.C., Stephens, M., and Gilad, Y. (2015). The genetic architecture of gene expression levels in wild baboons. Elife *4*, e04729.
61. Meissner, A., Gnirke, A., Bell, G.W., Ramsahoye, B., Lander, E.S., and Jaenisch, R. (2005). Reduced representation bisulfite sequencing for comparative high-resolution DNA methylation analysis. Nucleic acids research *33*, 5868-5877.
62. Boyle, P., Clement, K., Gu, H., Smith, Z.D., Ziller, M., Fostel, J.L., Holmes, L., Meldrim, J., Kelley, F., and Gnirke, A. (2012). Gel-free multiplexed reduced representation bisulfite sequencing for large-scale DNA methylation profiling. Genome biology *13*, R92.
63. Krueger, F. (2012). Trim Galore: a wrapper tool around Cutadapt and FastQC to consistently apply quality and adapter trimming to FastQ files, with some extra functionality for MspI-digested RRBS-type (Reduced Representation Bisufite-Seq) libraries. URL http://www.bioinformatics.babraham.ac.uk/projects/trim_galore/.
64. Xi, Y., and Li, W. (2009). BSMAP: whole genome bisulfite sequence MAPping program. BMC bioinformatics *10*, 232.
65. Krueger, F. (2015). Trim Galore!: A wrapper tool around Cutadapt and FastQC to consistently apply quality and adapter trimming to FastQ files. (0.4).
66. Hastie, T., Tibshirani, R., Narasimhan, B., and Chu, G. (2001). impute: Imputation for microarray data. Bioinformatics *17*, 520-525.
67. Friedman, J., Hastie, T., and Tibshirani, R. (2009). glmnet: Lasso and elastic-net regularized generalized linear models. R package version *1*.
68. Friedman, J., Hastie, T., and Tibshirani, R. (2010). Regularization paths for generalized linear models via coordinate descent. Journal of statistical software *33*, 1.
69. Snyder-Mackler, N., Sanz, J., Kohn, J.N., Brinkworth, J.F., Morrow, S., Shaver, A.O., Grenier, J.-C., Pique-Regi, R., Johnson, Z.P., and Wilson, M.E. (2016). Social status alters immune regulation and response to infection in macaques. Science *354*, 1041-1045.
70. Altmann, J., Schoeller, D., Altmann, S.A., Muruthi, P., and Sapolsky, R.M. (1993). Body size and fatness of free‐living baboons reflect food availability and activity levels. American Journal of Primatology *30*, 149-161.
71. Silk, J.B., Beehner, J.C., Bergman, T.J., Crockford, C., Engh, A.L., Moscovice, L.R., Wittig, R.M., Seyfarth, R.M., and Cheney, D.L. (2010). Strong and consistent social bonds enhance the longevity of female baboons. Current Biology *20*, 1359-1361.
72. Hausfater, G., Altmann, J., and Altmann, S. (1982). Long-term consistency of dominance relations among female baboons (Papio cynocephalus). Science *217*, 752-755.
73. Archie, E.A., Altmann, J., and Alberts, S.C. (2014). Costs of reproduction in a long-lived female primate: injury risk and wound healing. Behavioral ecology and sociobiology *68*, 1183-1193.
74. Beehner, J.C., Onderdonk, D.A., Alberts, S.C., and Altmann, J. (2006). The ecology of conception and pregnancy failure in wild baboons. Behavioral Ecology *17*, 741-750.
75. Altmann, J., and Alberts, S.C. (2003). Intraspecific variability in fertility and offspring survival in a nonhuman primate: behavioral control of ecological and social sources. In Offspring: The Biodemography of Fertility and Family Behavior, K.W. Wachter

754 and R.A. Bulatao, eds. (Washington, DC: The National Academies Press).
755 76. Altmann, J., Hausfater, G., and Altmann, S.A. (1988). Determinants of Reproductive
756 Success in Savannah Baboons, Papio cynocephalus. In Reproductive Success: Studies
757 of Individual Variation in Contrasting Breeding Systems, T.H. Clutton-Brock, ed.
758 (Chicago: The University of Chicago Press).
759 77. Charpentier, M., Tung, J., Altmann, J., and Alberts, S. (2008). Age at maturity in wild
760 baboons: genetic, environmental and demographic influences. Molecular Ecology *17*,
761 2026-2040.
762 78. Altmann, J., Altmann, S.A., and Hausfater, G. (1978). Primate infant's effects on
763 mother's future reproduction. Science *201*, 1028-1030.
764 79. Altmann, J., and Alberts, S.C. (2003). Variability in reproductive success viewed from
765 a life‐history perspective in baboons. American Journal of Human Biology *15*, 401-
766 409.
767 80. Lea, A.J., Learn, N.H., Theus, M.J., Altmann, J., and Alberts, S.C. (2014). Complex
768 sources of variance in female dominance rank in a nepotistic society. Animal
769 behaviour *94*, 87-99.
770 81. Vilgalys, T.P., Rogers, J., Jolly, C.J., Mukherjee, S., and Tung, J. (2018). Evolution of
771 DNA methylation in Papio baboons. Molecular biology and evolution *36*, 527-540.
772 82. Irizarry, R.A., Ladd-Acosta, C., Wen, B., Wu, Z., Montano, C., Onyango, P., Cui, H., Gabo,
773 K., Rongione, M., and Webster, M. (2009). The human colon cancer methylome
774 shows similar hypo-and hypermethylation at conserved tissue-specific CpG island
775 shores. Nature genetics *41*, 178.
776 83. Consortium, E.P. (2012). An integrated encyclopedia of DNA elements in the human
777 genome. Nature *489*, 57.
778